Malaysian Journal of Analytical Sciences (MJAS)
Published by Malaysian Analytical Sciences Society

PHYSICAL AND CHEMICAL PROPERTIES ON REDUCTION BEHAVIOUR OF CHROMIUM DOPED TO MOLYBDENUM OXIDE IN CARBON MONOXIDE ENVIRONMENT

(Sifat Fizikal dan Kimia terhadap Tindak Balas Penurunan Kromium yang Didopkan kepada Molibdenum Oksida di dalam Persekitaran Karbon Monoksida)

Nur Syakirah Abdul Rahim[1], Alinda Samsuri[2,3*], Mohd Nor Latif [4,5], Maratun Najiha Abu Tahari[6], Fairous Salleh[6], Tengku Shafazila Tengku Saharuddin[7], Norliza Dzakaria[8], and Muhammad Rahimi Yusop[6]

[1]Faculty of Defence Science and Technology, Universiti Pertahanan Nasional Malaysia, Kem Perdana Sungai Besi, 57000 Kuala Lumpur, Malaysia
[2]Centre for Tropicalization (CENTROP), Universiti Pertahanan Nasional Malaysia, Kem Perdana Sungai Besi, 57000 Kuala Lumpur, Malaysia
[3]Department of Chemistry and Biology, Centre for Defence Foundation Studies, Universiti Pertahanan Nasional Malaysia, Kem Perdana Sungai Besi, 57000 Kuala Lumpur, Malaysia
[4]GENIUS@Pintar National Gifted Centre, Universiti Kebangsaan Malaysia, 43600 Bangi, Selangor, Malaysia
[5]Research Centre for Sustainable Process Technology (CESPRO), Faculty of Engineering and Built Environment, Universiti Kebangsaan Malaysia, 43600 Bangi, Selangor, Malaysia
[6]Department of Chemical Sciences, Faculty of Science and Technology, Universiti Kebangsaan Malaysia, 43600 Bangi, Selangor, Malaysia
[7]Faculty of Science and Technology, Universiti Sains Islam Malaysia, Bandar Baru Nilai, 71800 Nilai, Negeri Sembilan, Malaysia
[8]School of Chemistry and Environment, Faculty of Applied Sciences, Universiti Teknologi MARA, Cawangan Negeri Sembilan, Kampus Kuala Pilah, Pekan Parit Tinggi, 72000 Kuala Pilah, Negeri Sembilan, Malaysia

**Corresponding author: alinda@upnm.edu.my*

Received: 7 September 2022; Accepted: 9 December 2022; Published: 19 April 2023

Abstract

This study aimed to investigate the influence of added chromium on the physical and chemical reduction behavior of molybdenum trioxide (MoO_3) in a carbon monoxide (CO) environment. The reduction behavior of the sample was evaluated by using temperature-programmed reduction (TPR), and the phases produced by the reduced samples were analyzed using X-ray diffraction spectroscopy (XRD) and field emission scanning electron microscopy (FESEM). The TPR study was conducted using two reduction modes: non-isothermal reduction at 700°C with 20 vol. % of CO in nitrogen (N_2), followed by isothermal reduction at 700°C for an additional 60 min. The TPR profile showed that the reduction of doped and undoped MoO_3 was preceded by two reduction stages ($MoO_3 \rightarrow Mo_4O_{11} \rightarrow MoO_2$), wherein, the reduction of doped MoO_3 starting at a lower temperature (380°C-500°C) than that of undoped MoO_3 (550°C). Additionally, based on XRD analysis, it was shown that the conversion of MoO_3 to MoO_2 under CO generated an intermediate product known as Mo_4O_{11}. It is discovered that, increasing the concentration of chromium doped to MoO_3 enhanced the reducibility of oxide due to the rapid production of MoO_2 phases at T: 380ºC. Further heating under CO atmosphere, carbide species built up in the form of Mo_2C rather than metallic Mo which might be due to excess of CO exposure to the surface layer of oxide.

Keywords: reduction, molybdenum oxide, carbon monoxide, chromium

Abstrak

Kajian ini bertujuan untuk menyiasat pengaruh penambahan kromium terhadap sifat fizikal dan kimia semasa penurunan molibdenum trioksida (MoO_3) dalam persekitaran karbon monoksida (CO). Tingkah laku penurunan sampel dinilai menggunakan teknik suhu penurunan berprogram (TPR), dan fasa yang dihasilkan oleh sampel yang diturunkan dianalisis menggunakan pembelauan sinar-X (XRD) dan pancaran medan mikroskopi elektron pengimbasan (FESEM). Kajian TPR telah dijalankan menggunakan dua mod penurunan: penurunan bukan isoterma pada 700°C dengan 20 vol. % CO dalam nitrogen (N_2), diikuti dengan pengurangan isoterma pada 700°C selama 60 minit. Keputusan TPR menunjukkan bahawa penurunan MoO_3 terdop dan tidak terdop didahului oleh dua peringkat penurunan iaitu ($MoO_3 \rightarrow Mo_4O_{11} \rightarrow MoO_2$) dengan penurunan MoO_3 terdop bermula pada suhu yang lebih rendah (380°C-500°C) berbanding MoO_3 tidak terdop (550°C). Di samping itu, telah ditentukan bahawa penurunan MoO_3 kepada MoO_2 dengan CO telah menghasilkan produk perantaraan yang dipanggil Mo_4O_{11} berdasarkan analisis sampel yang diturunkan menggunakan XRD. Telah didapati bahawa, peningkatan kepekatan kromium yang didopkan kepada MoO_3 telah meningkatkan penurunan oksida dengan pembentukan fasa MoO_2 yang lebih cepat pada T: 380ºC. Pemanasan berpanjangan di dalam persekitaran CO menyebabkan pembentukan spesies karbida dalam bentuk Mo_2C dan bukannya logam Mo yang mungkin disebabkan oleh pendedahan berlebihan CO pada lapisan permukaan oksida.

Kata kunci: Penurunan, molibdenum oksida, karbon monoksida, kromium

Introduction

Molybdenum oxide (MoO_3) has a density of 4.692 g/cm^3 and a melting point of 1068K (795°C), making it a viable source of Mo for direct alloying steel making or the manufacture of ferromolybdenum processes [1]. Because it helps quenched and tempered steels to become harder and more resilient, molybdenum is a valuable alloying agent. It also makes the steel more durable at high temperatures [2]. Electrodes for heated glass furnaces, nuclear energy applications, missile and aeroplane parts, the manufacturing of tungsten, glass to metal sealing, and colloidal form as a lubricant additive are all uses for molybdenum. As a catalyst, it can also be used in the refining of petroleum [3]. Additionally, the reduction of suitable reacting agents, such as hydrogen and carbon monoxide, is a necessary step in the synthesis of metallic molybdenum [4]. Generally, the generation of volatile molybdenum species produced at high temperatures is minimized by using the two-stage flow scheme ($MoO_3 \rightarrow MoO_2$, $MoO_2 \rightarrow Mo$). In a single-stage conversion of the molybdenum precursor, molybdenum must also be obtained through a separate method [5].

These days, hydrogen is used as a crucial reducing agent in the chemical sector. To produce pure molybdenum metal, the reduction process that uses hydrogen as a reducing agent goes through a two-step chemical reduction procedure [6]. MoO_3 is converted to MoO_2 in the first step of this reaction, which takes place at a lower temperature (450°C-650°C) [7]. MoO_2 is further reduced to metallic molybdenum during the second reduction step. The temperature range used for this technique is 1000°C-1100°C. Additionally, a critical step in the formation of metallic molybdenum is the reduction of MoO_3 to MoO_2. According to Wang et al. [8], MoO_3 is reduced to MoO_2 by using hydrogen as a reducing agent which consisting of two reduction processes, with the production of the intermediate phase Mo_4O_{11} occurring first before MoO_2.

Carbon can be used as a reducing agent to produce pure molybdenum as a choice. This technique comprises a high-temperature (600°C-1200°C) interaction between MoO_3 and carbon [9]. Additionally, the use of carbon in reduction is efficient because the reaction between metal oxide and carbon results in a gas that can be easily separated from the solid reaction product [10]. Carbon monoxide (CO), in addition to hydrogen and carbon, has started to be utilized as a reducing agent. However, just a few studies have investigated by using CO as a reducing agent to reduce MoO_3. Additionally, the use of chromium as an adjuvant has been extensively studied by researchers to increase the catalyst low-temperature reducibility and catalytic activity [11]. When chromium is added as a precursor, gas sensing for carbon monoxide can be improved at a relatively low temperature, according to Habib et al. [12].

In this study, the reduction behavior and degree of reduction of the molybdenum species were examined in an atmosphere with 20 vol. % of CO in N_2. The goal of this study was to identify the appropriate way to increase the reducibility of MoO_3 by adding chromium, including the best reduction temperatures. In addition, the temperature-programmed reduction (TPR) method was used to characterize the chromium-doped MoO_3 and analyze its reduction behavior in comparison to undoped species.

Materials and Methods

Materials

Commercially pure MoO_3 powder and chromium (III) nitrate, $Cr(NO_3)_3$, which were provided by BDH Chemicals Ltd. and Sigma Aldrich Chemical, respectively, served as the starting ingredients. Moreover, the impregnation procedure used ethanol, C_2H_6O (99.5%) from Systerm® as the solvent. In addition, Linde provided the gas mixture with 20 vol. % of CO in N_2.

Catalyst preparation

An aqueous solution containing chromium cation additives was used to impregnate MoO_3 powder to prepare the chromium doped with molybdenum oxide. Chromium was added in amounts of ($x = 3, 9, 15$) mol % of the total metal cation. Then, all prepared samples were dissolved in a mixture of distilled water and ethanol at 40°C while stirred vigorously for 4 h at room temperature (24ºC) to form a viscous mixture. The impregnated samples were first oven dried at 110°C overnight before being calcined for 4 h in air at 400°C. The doped catalyst was denoted as x Cr-MoO_3, ($x = 3, 9, 15\%$) while for undoped catalyst was denoted as MoO_3.

Temperature-programmed reduction

Using a Micromeritic Autochem 2920 Chemisorption Analyzer apparatus, the temperature-programmed reduction (TPR) method was used to analyze the total reduction of the undoped and doped MoO_3. With a flow rate of 20 mL min^{-1}, mixed gases containing 20 vol. % of CO and 80 vol. % of N_2 were fed into the micro reactor as the reducing gas (STP). Samples of 50 mg were heated at a rate of 10°C min^{-1} to 700°C. Then, an isothermal mode of reduction was used when temperature reached at 700°C and prolong the reaction from 30 min to 60 min. All analyses were identified by a thermal conductivity detector (TCD).

Characterizations

The physicochemical properties were characterized by X-Ray Diffraction (XRD), using the Cu Kα X-ray radiation source (40 kV, 40 mA) in the XRD Bruker AXS D8 (Advance type) to record the 2θ diffraction angle from 10° to 80° at wavelength ($\lambda = 0.154$ nm). Surface area and porosity were characterized by using Brunauer-Emmett-Teller (BET) utilizing the Micromeritics ASAP 2020 equipment. The samples underwent degassing at 200°C for 4 h, before treatment under liquid N_2 at -198ºC. Following that, the surface morphology of the reduced MoO_3 was studied using a Carl Zeiss Merlin field emission scanning electron microscope (FESEM).

Results and Discussion

XRD analysis of the structural properties of doped and undoped MoO_3

The XRD patterns of undoped and doped MoO_3 with various loadings of chromium were displayed after calcined at 400°C for 4 hours (Figure 1). It shows that undoped MoO_3 patterns largely existed as MoO_3 (JCPDS 05-0508) [4]. Nevertheless, the addition of chromium to MoO_3 had little effect on their mesoporous structure, as summarised in Table 1. About the display of chromium molybdenum oxide, $Cr_2(MoO_4)_3$, just a small difference in XRD patterns was noticed (JCPDS 77-5936). Moreover, the intensity of MoO_3 peaks decreased especially for MoO_3 with higher chromium loadings. The 2θ range of MoO_3 peaks showed many new $Cr_2(MoO_4)_3$ diffraction peaks at 15 mol % of chromium loading, which demonstrated that the impregnation of chromium on the MoO_3 was truly successful at range of 2θ = 20°-40°. The interference of chromium element which altered the lattice constant of

MoO_3, was primarily responsible for the evolution of diffraction peaks. This can be attributed to the differences in atomic radius of molybdenum and chromium, which can alter the lattice parameters and spacing. It was found that the difference in atomic size, electronic interaction, and magnetic spin relations between the solute and its solvent atoms (Cr-MoO_3) which all were contributed to the lattice distortions [13].

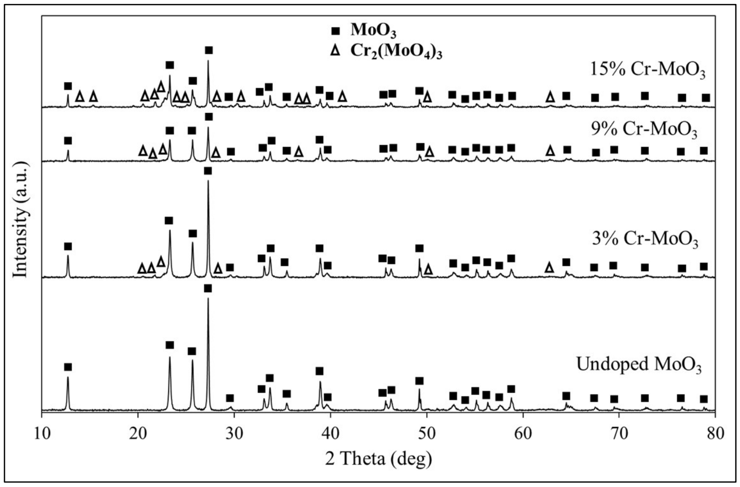

Figure 1. XRD patterns of undoped MoO_3 and chromium-doped of MoO_3 at various loadings after calcinations at 400 °C for 4 h

BET analysis from the N_2 adsorption isotherm for structural properties

The analysis of N_2 adsorption-desorption isotherm at 77 K was used to identify the effect of the impregnation on the textural characteristics of MoO_3. Table 1 provides information about the textural properties of doped MoO_3 including BET surface area, total pore volume, and average pore size width. The surface area (BET), pore volume, and pore size of doped MoO_3 decreased as increasing the amount of chromium concentration of MoO_3 (6.85 m²/g) > 3% Cr-MoO_3 (5.91 m²/g) > 9% Cr-MoO_3 (3.28 m²/g) > 15% Cr-MoO_3 (2.26 m²/g). Decreasing of surface area of doped samples might be due to the ion-exchange that caused the low dispersion of Mo oxide after addition of chromium, which agreed with the decreasing of XRD peak intensity of MoO_3 at $2\theta = 27^\circ$ (Figure 1). Mesopore sizes decreased from 20.4 nm in undoped MoO_3 to 18.1 nm, 15.4 nm, and 14.3 nm with 3 mol %, 9 mol %, and 15 mol % of chromium addition, respectively. Besides, the cumulative pore volume (cm³/g) in Table 1 demonstrated that the overall pore volume for undoped MoO_3 was 0.035 cm³/g, and by increased the amount of chromium added had reduced the pore volume to 0.027 cm³/g, 0.013 cm³/g, and 0.008 cm³/g, respectively. These demonstrated that the chromium layer present on the pore surfaces of MoO_3 had been the reason for the reduced pore size and pore volume of all doped MoO_3. Therefore, MoO_3 loaded with a higher percentage of chromium possessed smaller pore sizes and a decreased in pore volume. The decreasing of pore size and volume as increasing the addition of chromium concentration were due to the Cr salt filled in the pore of Mo oxide.

Table 1. BET analysis of chromium-doped of MoO_3 and undoped MoO_3

Catalyst	Surface Area (m²/g)	Pore Size (nm)	Pore Volume (cm³/g)
Undoped MoO_3	6.85	20.4	0.035
3% of Cr-MoO_3	5.91	18.1	0.027
9% of Cr-MoO_3	3.28	15.4	0.013
15% of Cr-MoO_3	2.26	14.3	0.008

TPR analysis of chemical properties

The TPR analysis was used to establish the reduction properties of each sample. The TPR profiles of prepared samples with *x* = 3, 9, 15 mol % of Cr-MoO_3 and undoped MoO_3 in a non-isothermal reduction under 20 vol. % of CO in N_2 and a continuation in an isothermal reduction mode at 700°C for 60 min are shown in Figure 2. Non-isothermal reduction at 700°C was added to the reduction system to prevent the production of alloy-fused mass, if the complete reduction to MoO_2 was not accomplished at a temperature below the melting point of MoO_3 (795°C) [6]. There were three reduction phases involved in the reduction of pure MoO_3 to Mo: Mo^{6+} to Mo^{5+}, Mo^{5+} to Mo^{4+}, and Mo^{4+} to Mo^0 [8]. By referring to the results obtained from the reduction of undoped and doped MoO_3 with chromium, the TPR profiles thus displayed nearly identical patterns by presenting two reduction peaks (denoted I and II), whereby the first peak owing to the reduction of MoO_3 to Mo_4O_{11} and the second peak represented the reduction of Mo_4O_{11} to MoO_2 [14].

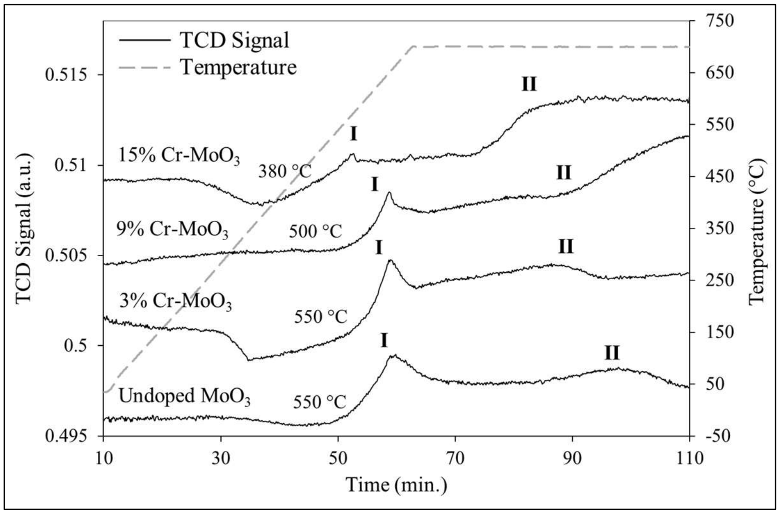

Figure 2. TPR profiles of undoped MoO_3 and chromium-doped of MoO_3

According to Dang et al. [5], the CO consumption peaks of undoped MoO_3 that began at roughly 550°C indicated that the initial phase of reduction was a Phase I as the production of Mo_4O_{11}. Due to sample modifications that took place 40 min after the isothermal reduction process began at 700°C, new peaks designated as Phase II were noticed. These peaks represented the second phase reduction of Mo_4O_{11} to MoO_2. Nonetheless, the addition of chromium to MoO_3 provided different information about the reducibility of MoO_3. The TPR results showed that the interaction between different loadings of chromium to MoO_3 decreased the reduction temperature and all peaks were shifted to a lower temperature. Besides, doping with chromium generated some amount of oxygen release and lowered the TPR reduction temperature [15].

However, TPR profile (Figure 2) also clearly shows two dominant peaks of doped MoO_3 designated as I and II. By adding 3 mol % of chromium, the reduction temperature of doped MoO_3 remained unchanged at early stage of reduction (I) as undoped MoO_3 at 550ºC. However, it was observed during the isothermal reaction, the reduction peak (II) appeared faster as compared to undoped MoO_3. Then, at 60 min and 90 min of reduction time, respectively showed the TPR profile for 9% of Cr-MoO_3 was designated as I and II. Peak I was observed at 650ºC represented the reduction of MoO_3 to Mo_4O_{11}, while peak II appeared after 20 min of isothermal reduction, which represented the complete reduction of MoO_2. At higher concentration of 15% of Cr-MoO_3, peak I and peak II shifted to a lower reduction (380°C and 10th min) as compared to undoped and lower Cr concentration. Besides, for the reduction of doped MoO_3 with 15 mol % of chromium, the TPR profile was almost similar as it portrayed two peaks, whereby the first reduction peak was noted at about 380°C, which was lower than undoped MoO_3 (550°C), whereas the second peak began its formation at the 10th minute of isothermal reduction. As shown by the XRD analysis in Figure 4, increasing the isothermal reduction could lead to the synthesis of Mo_2C rather than metallic molybdenum [16].

It was evident that the addition of chromium to MoO_3 might have a major impact on the powder reduction by increasing the powder reducibility and oxygen storage capacity. Additionally, there were some changes in the coordination environment of molybdenum and the strength of Mo-O bonds because of the strong interaction between chromium ions and molybdenum ions in the samples [17]. In comparison to conventional Ni catalysts, Ni-Cr catalysts often exhibited substantially stronger anti-coking and anti-sintering capabilities, as well as much higher catalytic activity and stability. The smaller Ni particle size, the enhancing influence of Cr, and the increased sorption capacities for both H_2 and CO absorption are all thought to be the causes of the better catalytic performance [18] and indirectly causes the enhancement of reducibility of oxide. Next, to determine the changes in the samples, the residual obtained after TPR reduction was studied by recording the XRD pattern and examining the morphological change by using FESEM.

Crystallinity studies

The XRD profile of spent catalysts during non-isothermal reduction at 700ºC are shown in Figure 3. Major peaks of unreduced MoO_3 and the intermediary phase of Mo_4O_{11} (JCPDS 84-0687) were visible in the XRD patterns of reduced undoped MoO_3 (JCPDS 74-7383) [19]. The XRD pattern was also nearly identical to that of undoped MoO_3, with Mo_4O_{11} forming as an intermediate phase. Mo_4O_{11} was produced during the reduction of MoO_3 to MoO_2, according to Dang et al. [5]. This finding proved the formation of Mo_4O_{11} as predicted in TPR profile (Figure 2). Meanwhile, with the addition of 9 mol % of chromium, the MoO_3 phase almost disappeared and the Mo_4O_{11} phase was present as the dominant species. However, the addition of 9 mol % of chromium, showed a low intensity for the crystalline phase of Mo_4O_{11} due to the formation of $Cr_2(MoO_4)_3$ alloy (JCPDS 078-1654). Then, for the addition of 15 mol % of chromium, the patterns revealed that the reduction product was rather the same as the addition of 9 mol % of chromium with the major forms of Mo_4O_{11} and a few peaks of $Cr_2(MoO_4)_3$ alloy. However, no remaining unreduced MoO_3 peaks had been observed. Therefore, it had been discovered that adding more chromium might speed up reduction process of MoO_3.

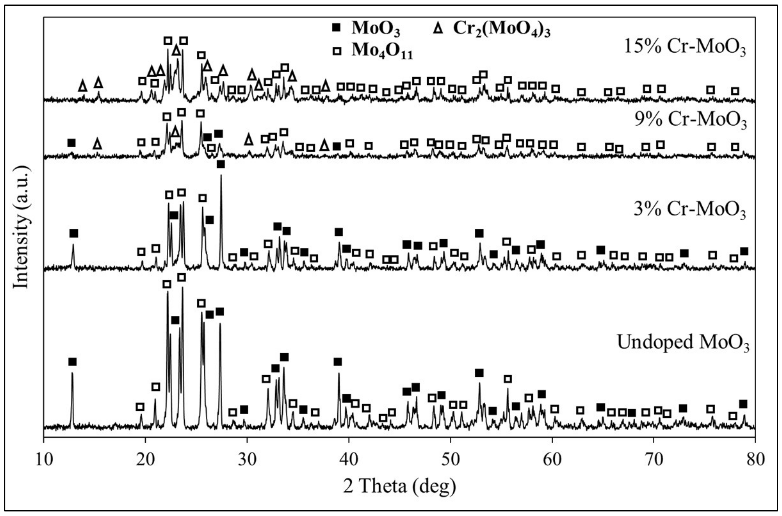

Figure 3. XRD patterns of 20 vol. % of CO in N_2 of non-isothermal reduction at 700°C

Figure 4 showed the XRD diffraction which carried out in isothermal mode for 60 min by using 20 vol. % of CO at 700°C to further reduce to MoO_2 phases. After 60 min of isothermal reduction, all samples had completely reduced to the MoO_2 phase (JCPDS 76-1807) [20]. In addition, the peaks that represented $Cr_2(MoO_4)_3$ alloy had completely disappeared in 9 mol % and 15 mol % of chromium-doped of MoO_3 samples after isothermal reduction. However, the increased addition of chromium showed that the low crystallinity of MoO_2 synthesis was affected by the formation of $Cr_2(MoO_4)_3$ alloy at range of 2θ = 20°-40° (Figure 1) which enhanced the reduction performance of MoO_3. According to the formation of Mo_2C (JCPDS 071-0242) in 15 % of Cr-MoO_3 samples during isothermal reduction at 700°C for 60 min, carbide was formed when excessive CO was added to the MoO_2 phase. This finding was in agreement with Wang et al. [21] regarding the formation of Mo_2C.

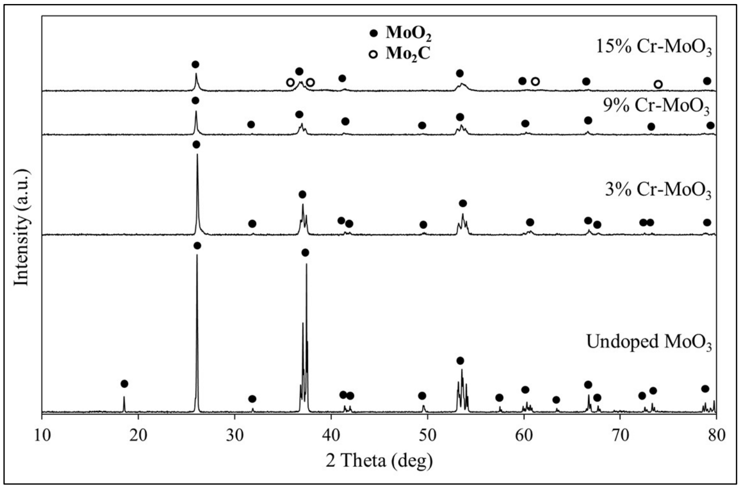

Figure 4. shows the XRD patterns of non-isothermal reduction in 20 vol. % of CO in N_2 up to 700°C and continued in isothermal mode at 700°C for 60 min

Apart from that, it can be concluded that the reduction step involved in the samples had been in the sequence of $MoO_3 \rightarrow Mo_4O_{11} \rightarrow MoO_2$ [8]. With the addition of chromium, the reducibility of MoO_3 was enhanced by changing the physiochemical properties of MoO_3, by the formation of $Cr_2(MoO_4)_3$ alloy which was confirmed by XRD analysis. As a result, it made the transition of MoO_3 to MoO_2 easier. The formation of Mo_2C instead of metallic molybdenum occurred when excessive CO was supplied to the MoO_2 phase, which was in line with the report by Alinda et al. [16] that the presence of excessive CO in the reduction process caused the formation of carbon on the external surface of Mo layer.

Morphological studies

Based on the TPR and XRD results, FESEM analysis was employed to identify new phases after the reduction process. The undoped MoO_3 morphology, according to Alinda et al. [4] is characterised by agglomerations of non-porous grains in vast numbers and with non-uniform sizes. However, as the reduction process continued, the resulting structures took on the appearance of a thin plate with an asymmetrical shape, demonstrating the rapid formation of MoO_2 phase from Mo_4O_{11} [4]. Figure 5 depicts the morphological change that occurred during the reduction of MoO_3 with various chromium loadings in 20 vol. % of CO in N_2 up to 700°C and proceeded with isothermal reduction for 60 min at 700°C.

The morphology of MoO_3 doped with 3 mol % of chromium is depicted in Figure 5(a). Figure 5(a) shows, no chromium particles had been observed on the MoO_3 surface. However, referring to BET results presented in Table 1, the surface areas eventually decreased. It revealed that the chromium added had successfully penetrated the MoO_3 pores. After the reduction process, the MoO_2 phase with the plate-like particles and coated with small particles had been observed, as illustrated in Figure 5 (b). Other than that, as shown in Figure 5 (c) and Figure 5 (e), when the addition of chromium was increased to 9 mol % and 15 mol %, small particles had been observed on the surface of MoO_3. It seemed that the MoO_3 pores were filled with chromium and excessive chromium was attached to the surface of MoO_3, which was in agreement with the decreasing of surface area (BET) result. However, following a reduction, the MoO_2 phase developed plate-like particles with smaller particles dispersed on its surface, as depicted in Figure 5 (d) and Figure 5 (f). Another intriguing finding that can be seen in Figure 5 is the additional phase formation that occurred on the surface of the 15% of Cr-MoO_3 sample because of carbon deposition on MoO_2 surface rather than further Mo_2C production [1].

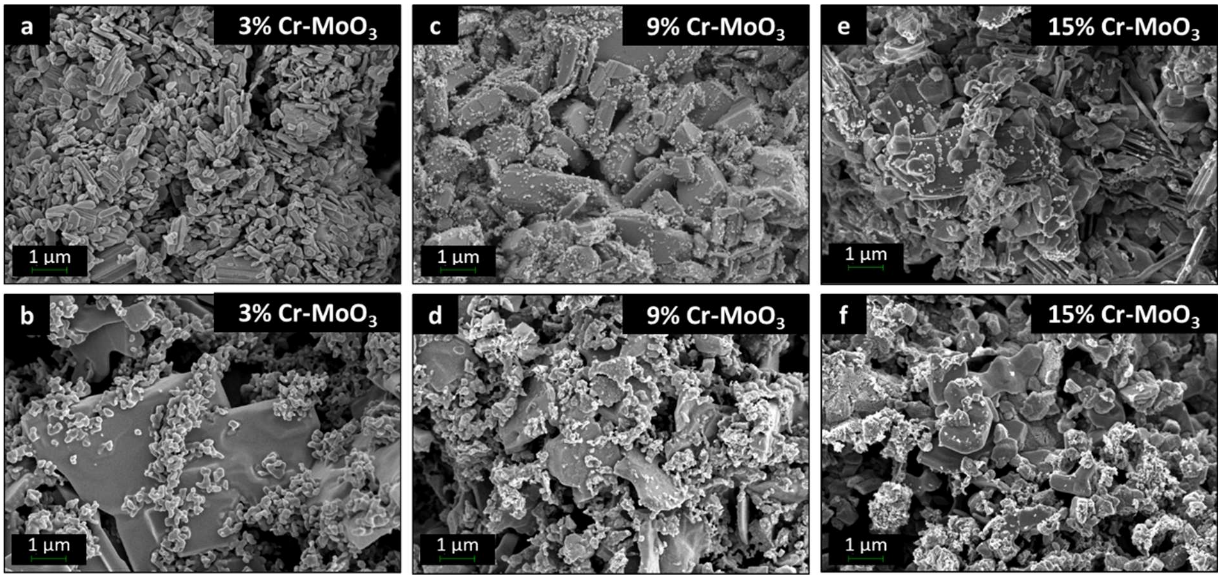

Figure 5. FESEM images before (top) and after (bottom) reduction in magnification 3,000X

Conclusion

Utilizing the TPR approach, the reduction behavior of chromium-doped and undoped MoO_3 was examined, compared, and characterized by XRD and FESEM analyses. The existence of $Cr_2(MoO_4)_3$ alloy on MoO_3 was demonstrated by the XRD data, which had the impact of accelerating the reduction process by reducing the temperature at which MoO_3 was reduced to the MoO_2 phase. As a result, adding chromium produced a two-step reduction process ($MoO_3 \rightarrow Mo_4O_{11} \rightarrow MoO_2$) that was comparable to MoO_3 that was not doped. Furthermore, better reducibility of Cr-MoO_3 was also due to the physicochemical changes on MoO_3 through the formation of successful intercalation of chromium onto the surface of MoO_3, which was further confirmed with the decreased in the surface area for chromium-doped MoO_3. However, excessive CO was added to the MoO_2 phase, Mo_2C would instead develop as opposed to metallic molybdenum.

Acknowledgement

The project was funded by research grant number RACER/1/2019/STG07/UPNM/2 from the Ministry of Higher Education (MOHE) of Malaysia, UPNM/2022/GPPP/SG/10 from Universiti Pertahanan Nasional Malaysia (UPNM), and Universiti Kebangsaan Malaysia (UKM), as well as the Centre of Research and Innovation Management (CRIM) of UKM, Malaysia for the instruments and facilities.

References

1. Wang, L., Bu, C. Y., Zhang, G. H., Wang, J. S., and Chou, K. C. (2017). Study of the reduction of industrial grade MoO_3 powders with CO or CO-CO_2 gases to prepare MoO_2. *Metallurgical and Materials Transactions B: Process Metallurgy and Materials Processing Science,* 48(4): 2047-2056.
2. Chen, X. R., Zhai, Q. J., Dong, H., Dai, B. H., and Mohrbacher, H. (2020). Molybdenum alloying in cast iron and steel. *Advances in Manufacturing*, 8(1): 3-14.
3. Jaf, Z. N., Miran, H. A., Jiang, Z. T. and Altarawneh, M. (2021). Molybdenum nitrides from structures to industrial applications. *Reviews in Chemical Engineering*, 2021:1015.
4. Samsuri, A., Latif, M. N., Shamsuddin, M. R., Salleh, F., Abu Tahari, M. N., Tengku Saharuddin, T. S., Dzakaria, N., and Yarmo, M. A. (2021). Studies on influence of hydrogen and carbon monoxide concentration on reduction progression behavior of molybdenum oxide catalyst. *International Journal of Hydrogen Energy,* 46(48): 24831-24844.
5. Dang, J., Zhang, G. H., Chou, K. C., Reddy, R. G., He, Y., and Sun, Y. (2013). Kinetics and mechanism of hydrogen reduction of MoO_3 to MoO_2. *International Journal of Refractory Metals and Hard Materials*, 41: 216-223.
6. Saghafi, M., Heshmati-Manesh, S., Ataie, A., and Khodadadi, A. A. (2012). Synthesis of nanocrystalline molybdenum by hydrogen reduction of mechanically activated MoO_3. *International Journal of Refractory Metals and Hard Materials*, 30(1): 128-132.
7. Enneti, R. K., and Wolfe, T. A. (2012). Agglomeration during reduction of MoO_3. *International Journal of Refractory Metals and Hard Materials,* 31: 47-50.
8. Wang, J., Ren, Z., Liu, W., Gao, F., and Zhou, M. (2009). Effects of RE_2O_3 doping on the reduction behavior of molybdenum oxide and properties of molybdenum powder. *International Journal of Refractory Metals and Hard Materials*, 27(1): 155-158.
9. Saghafi, M., Ataie, A., and Heshmati-Manesh, S. (2011). Effects of mechanical activation of MoO_3/C powder mixture in the processing of nano-crystalline molybdenum. *International Journal of Refractory Metals and Hard Materials*, 29(4): 419-423.
10. Wu, S., Zhou, C., Doroodchi, E., Nellore, R., and Moghtaderi, B. (2018). A review on high-temperature thermochemical energy storage based on metal oxides redox cycle. *Energy Conversion and Management*, 168: 421–453.
11. Zhang, G., Liu, J., Xu, Y., and Sun, Y. (2018). A review of CH_4–CO_2 reforming to synthesis gas over Ni-based catalysts in recent years (2010–2017). *International Journal of Hydrogen Energy*, 43(32): 15030-15054.
12. Habib, I. Y., Tajuddin, A. A., Noor, H. A., Lim, C. M., Mahadi, A. H., and Kumara, N. T. R. N. (2019). Enhanced Carbon monoxide-sensing properties of Chromium-doped ZnO nanostructures. *Scientific Reports,* 9(1): 9207.
13. Wang, T., Chen, L. Q., and Liu, Z. K. (2007). Lattice parameters and local lattice distortions in FCC-Ni solutions. *Metallurgical and Materials Transactions A: Physical Metallurgy and Materials Science,* 38(3): 562-569.
14. Samsuri, A., Tengku Saharuddin, T. S., Salleh, F., Othaman, R., Mohamed Hisham, M. W., and Yarmo, M. A. (2016). Temperature programmed reduction and x-ray diffractometry studies of MoO_3 reduction by different concentrations of carbon monoxide. *Malaysian Journal of Analytical Sciences,* 20: 382-387.
15. Saharuddin, T. S. T., Samsuri, A., Salleh, F., Othaman, R., Kassim, M. bin, Mohamed Hisham, M. W., and Yarmo, M. A. (2017). Studies on reduction of chromium doped iron oxide catalyst using hydrogen and various concentration of carbon monoxide. *International Journal of Hydrogen Energy,* 42(14): 9077-9086.
16. Samsuri, A., Tengku Saharuddin, T. S., Salleh, F., Mohamed Hisham, M. W., Othaman, R., and Yarmo, M. A. (2015). Reduction of MoO_2 to metallic molybdenum via carburization and thermal process. *Advanced Materials Research,* 1087: 64-67.
17. Sun, T., Xu, L., Wei, S., Xiao, F., Li, Z., Fan, X., and Zhou, Y. (2020). Phase evolution of

hydrothermal synthesis oxide-doped molybdenum powders. *International Journal of Refractory Metals and Hard Materials,* 86: 105085.

18. Liu, Q., Zhong, Z., Gu, F., Wang, X., Lu, X., Li, H., Xu, G., and Su, F. (2016). CO methanation on ordered mesoporous Ni-Cr-Al catalysts: Effects of the catalyst structure and Cr promoter on the catalytic properties. *Journal of Catalysis*, 337: 221-232.
19. Samsuri, A., Salleh, F., Tengku Saharuddin, T. S., Othaman, R., Mohammad Hisham, M. W., and Yarmo, M. A. (2017). Effect of noble metal silver on the reduction behaviour of molybdenum oxide using carbon monoxide. *Materials Science Forum,* 888: 377-381.
20. Latif, M. N., Samsuri, A., Mohammad Hisham, M. W., and Yarmo, M. A. (2017). Reduction of molybdenum trioxide by using hydrogen. *Materials Science Forum*, 888: 404-408.
21. Wang, L., Zhang, G. H., and Chou, K. C. (2018). Preparation of Mo_2C by reducing ultrafine spherical β-MoO_3 powders with CO or CO-CO_2 gases. *Journal of the Australian Ceramic Society*, 54(1): 97-107.